Research Article | Vol. 25, No. 23 | 13 Nov 2017 | OPTICS EXPRESS 29356
Optics EXPRESS

Ppb-level detection of ammonia based on QEPAS using a power amplified laser and a low resonance frequency quartz tuning fork

YUFEI MA,[1,*] YING HE,[1] YAO TONG,[1] XIN YU,[1] AND FRANK K. TITTEL[2]

[1]National Key Laboratory of Science and Technology on Tunable Laser, Harbin Institute of Technology, Harbin 150001, China
[2]Department of Electrical and Computer Engineering, Rice University, 6100 Main Street, Houston, Texas 77005, USA
[*]mayufei@hit.edu.cn

Abstract: In this report, an ultra-high sensitive quartz-enhanced photoacoustic spectroscopy (QEPAS) based ammonia (NH_3) sensor using a power amplified diode laser and a low resonance frequency quartz tuning fork (QTF) was demonstrated for the first time. A fiber-coupled, continuous wave (CW), distributed feedback (DFB) diode laser with a watt level output power boosted by an erbium-doped fiber amplifier (EDFA) was used as the QEPAS excitation source. A QTF with a resonance frequency of 30.72 kHz was employed as an acoustic wave transducer. The modulation depth in the wavelength modulation spectroscopy (WMS) based QEPAS system was optimized theoretically and validated by experimental measurements. For the reported NH_3 sensor system, a 418.4 ppbv (parts per billion by volume) minimum detection limit at a NH_3 absorption line of 6533.4 cm^{-1} was achieved when the modulation depth was set to the optimum value of 0.188 cm^{-1}. The ppb-level detection sensitivity verified the design of the reported QEPAS method and makes it suitable for use in environmental monitoring and other applications.

OCIS codes: (280.3420) Laser sensors; (300.6260) Spectroscopy, diode lasers; (280.4788) Optical sensing and sensors.

References and links

1. L. R. Narasimhan, W. Goodman, and C. K. N. Patel, "Correlation of breath ammonia with blood urea nitrogen and creatinine during hemodialysis," Proc. Natl. Acad. Sci. U.S.A. **98**(8), 4617–4621 (2001).
2. V. P. Aneja, P. A. Roelle, G. C. Murray, J. Southerland, J. W. Erisman, D. Fowler, W. A. H. Asman, and N. Patni, "Atmospheric nitrogen compound II: emissions, transport, transformation, deposition and assessment," Atmos. Environ. **35**, 1903–1911 (2000).
3. K. W. van der Hoek, "Estimating ammonia emission factors in Europe: summary of the work of the UNECE ammonia expert panel," Atmos. Environ. **32**, 315–316 (1998).
4. G. P. Wyers, R. P. Otjes, and J. Slanina, "A continuous-flow denuder for the measurement of ambient concentration and surface-exchange fluxes of ammonia," Atmos. Environ. **27a**, 2085–2090 (1993).
5. M. P. Keuken, A. Wayers-Ijpelaan, J. J. Mols, R. P. Otjes, and J. Slanina, "The determination of ammonia in ambient air by an automated thermodenuder system," Atmos. Environ. **23**, 2177–2185 (1989).
6. R. Claps, F. V. Englich, D. P. Leleux, D. Richter, F. K. Tittel, and R. F. Curl, "Ammonia detection by use of near-infrared diode-laser-based overtone spectroscopy," Appl. Opt. **40**(24), 4387–4394 (2001).
7. M. E. Webber, D. S. Baer, and R. K. Hanson, "Ammonia monitoring near 1.5 µm with diode-laser absorption sensors," Appl. Opt. **40**(12), 2031–2042 (2001).
8. A. Elia, P. M. Lugarà, C. Di Franco, and V. Spagnolo, "Photoacoustic techniques for trace gas sensing based on semiconductor laser sources," Sensors (Basel) **9**(12), 9616–9628 (2009).
9. A. A. Kosterev, Y. A. Bakhirkin, R. F. Curl, and F. K. Tittel, "Quartz-enhanced photoacoustic spectroscopy," Opt. Lett. **27**(21), 1902–1904 (2002).
10. H. M. Yi, R. Maamary, X. M. Gao, M. W. Sigrist, E. Fertein, and W. D. Chen, "Short-lived species detection of nitrous acid by external-cavity quantum cascade laser based quartz-enhanced photoacoustic absorption spectroscopy," Appl. Phys. Lett. **106**, 101109 (2015).
11. J. P. Waclawek, H. Moser, and B. Lendl, "Compact quantum cascade laser based quartz-enhanced photoacoustic spectroscopy sensor system for detection of carbon disulfide," Opt. Express **24**(6), 6559–6571 (2016).
12. K. Liu, W. X. Zhao, L. Wang, T. Tan, G. S. Wang, W. J. Zhang, X. M. Gao, and W. D. Chen, "Quartz-enhanced photoacoustic spectroscopy of HCN from 6433 to 6613 cm^{-1}," Opt. Commun. **340**, 126–130 (2015).

#308055 https://doi.org/10.1364/OE.25.029356
Journal © 2017 Received 27 Sep 2017; revised 6 Nov 2017; accepted 7 Nov 2017; published 9 Nov 2017

13. M. Mordmüller, M. Köhring, W. Schade, and U. Willer, “An electrically and optically cooperated QEPAS device for highly integrated gas sensors,” Appl. Phys. B **119**, 111–118 (2015).
14. Y. F. Ma, X. Yu, G. Yu, X. D. Li, J. B. Zhang, D. Y. Chen, R. Sun, and F. K. Tittel, “Multi-quartz-enhanced photoacoustic spectroscopy,” Appl. Phys. Lett. **107**, 021106 (2015).
15. M. C. Wu, N. A. Olsson, D. Sivco, and A. Y. Cho, “A 970 nm strained-layer InGaAs/GaAlAs quantum well laser for pumping an erbium-doped optical fiber amplifier,” Appl. Phys. Lett. **56**, 221–223 (1990).
16. M. Nakazawa, Y. Kimura, and K. Suzuki, “Efficient Er^{3+}-doped optical fiber amplifier pumped by a 1.48 μm InGaAsP laser diode,” Appl. Phys. Lett. **54**, 295–297 (1989).
17. H. P. Wu, L. Dong, H. D. Zheng, X. L. Liu, X. K. Yin, W. G. Ma, L. Zhang, W. B. Yin, S. T. Jia, and F. K. Tittel, “Enhanced near-infrared QEPAS sensor for sub-ppm level H_2Sdetection by means of a fiber amplified 1582 nm DFB laser,” Sensor. Actuat. B **221**, 666–672 (2015).
18. H. P. Wu, A. Sampaolo, L. Dong, P. Patimisco, X. L. Liu, H. D. Zheng, X. K. Yin, W. G. Ma, L. Zhang, W. B. Yin, V. Spagnolo, S. T. Jia, and F. K. Tittel, “Quartz enhanced photoacoustic H_2S gas sensor based on a fiber-amplifier source and a custom tuning fork with large prong spacing,” Appl. Phys. Lett. **107**, 111104 (2015).
19. S. Borri, P. Patimisco, A. Sampaolo, M. S. Vitiello, H. E. Beere, D. A. Ritchie, G. Scamarcio, and V. Spagnolo, “Terahertz quartz enhanced photo-acoustic sensor,” Appl. Phys. Lett. **103**, 021105 (2013).
20. Y. Ma, R. Lewicki, M. Razeghi, and F. K. Tittel, “QEPAS based ppb-level detection of CO and N_2O using a high power CW DFB-QCL,” Opt. Express **21**(1), 1008–1019 (2013).
21. L. Dong, V. Spagnolo, R. Lewicki, and F. K. Tittel, “Ppb-level detection of nitric oxide using an external cavity quantum cascade laser based QEPAS sensor,” Opt. Express **19**(24), 24037–24045 (2011).
22. Z. Wang, Z. Li, and W. Ren, “Quartz-enhanced photoacoustic detection of ethylene using a 10.5 μm quantum cascade laser,” Opt. Express **24**(4), 4143–4154 (2016).
23. S. Schilt and L. Thevenaz, “Wavelength modulation photoacoustic spectroscopy: Theoretical description and experimental results,” Infrared Phys. Technol. **48**, 154–162 (2006).
24. S. Schilt, L. Thévenaz, and P. Robert, “Wavelength modulation spectroscopy: combined frequency and intensity laser modulation,” Appl. Opt. **42**(33), 6728–6738 (2003).
25. L. S. Rothman, I. E. Gordon, A. Barbe, D. C. Benner, P. F. Bernath, M. Birk, V. Boudon, L. R. Brown, A. Campargue, J.-P. Champion, K. Chance, L. H. Coudert, V. Dana, V. M. Devi, S. Fally, J.-M. Flaud, R. R. Gamache, A. Goldman, D. Jacquemart, I. Kleiner, N. Lacome, W. Lafferty, J.-Y. Mandin, S. T. Massie, S. N. Mikhailenko, C. E. Miller, N. Moazzen-Ahmadi, O. V. Naumenko, A. V. Nikitin, J. Orphal, V. I. Perevalov, A. Perrin, A. Predoi-Cross, C. P. Rinsland, M. Rotger, M. Simeckova, M. A. H. Smith, K. Sung, S. A. Tashkun, J. Tennyson, R. A. Toth, A. C. Vandaele, and J. Vander Auwera, “The HITRAN 2008 molecular spectroscopic database,” J. Quant. Spectrosc. Radiat. Transf. **110**, 533–572 (2009).

1. Introduction

Ammonia (NH_3) detection is widely used for industrial and environmental pollution monitoring, automotive exhaust analysis and medical diagnostics. For example, NH_3 can serve as a biomarker for liver and kidney disorders [1]. The main emission source of NH_3 is the use of animal manure and fertilizers for agriculture [2,3]. Typical concentrations of NH_3 in the atmospheric boundary layer range from <1 part per billion (ppb) by volume in the troposphere to parts per million (ppm) levels above animal waste sites and near animal sheds. Hence, there is a significant need for sensitive detection of NH_3 concentrations at ppb levels.

Laser absorption spectroscopy (LAS) has the advantages of fast response, non-invasive, highly sensitive and selective detection compared with other non-optical techniques for NH_3 detection [4,5]. As one of the most widely used LAS methods, tunable diode laser absorption spectroscopy (TDLAS) employing a multi-pass cell (MPC), where effective optical path length is extended to tens or even to hundreds of meters, typically allows to reach a detection limits of the analyte species at ppm or ppb levels [6,7]. However this type of sensor is usually bulky due to the large size of a MPC and the increased number of optical components that are needed for laser beam alignment. For example, in [6,7], the MPCs had physical length of 20 cm for NH_3 detection. Photoacoustic spectroscopy (PAS) is an alternative effective trace gas sensing technology which employs a broadband microphone for acoustic wave detection. However, most microphone-based PAS cells have a low resonance frequency (<2 kHz), which makes such cells more sensitive to environmental and sample gas flow noise [8]. Moreover, the Q-factor of typical PAS cell is low (<200) and the size of PAS cell is still considered to be too large.

A modification of conventional PAS is the quartz-enhanced photoacoustic spectroscopy (QEPAS) technique [9]. This technique uses a commercially available inexpensive, millimeter sized piezoelectric quartz tuning fork (QTF) as an acoustic wave transducer. The

Optics EXPRESS

high Q-factor (~10 000 at 1 atm; ~100 000 in vacuum) and narrow resonance frequency band of QTF improve the QEPAS selectivity and immunity to environmental acoustic noise [10,11]. The primary noise source of QEPAS is limited by the fundamental Johnson thermal noise of the QTF. An important advantage of QEPAS is that the performance of QEPAS-based sensors can be improved when the excitation laser power is increased, since the QEPAS detection sensitivity scales linearly with excitation laser power. This feature differs from other laser absorption spectroscopy such as TDLAS. Diode lasers are usually used in QEPAS based sensing systems due to their compactness and low cost [12–14]. However the output power of diode lasers is in the range of several milliwatts which limits the QEPAS detection performance. Optical fiber amplifiers, which are widely used in optical communications, can realize significant optical signal amplification. In a commercially available optical fiber amplifier, a short length of single-mode optical fiber is doped with rare-earth ions and is pumped by diode lasers. An erbium-doped fiber amplifier (EDFA) offers several advantages, such as high gain, low noise, polarization independence, and fiber compatibility [15,16]. An EDFA can be used to achieve amplification gain of more than 30 dB when an appropriate seed diode laser beam is injected and was successfully used in QEPAS based sensor systems [17,18]. Three operating wavelength bands (S band: 1450-1550 nm, C band: 1520-1570 nm, and L band: 1565-1610 nm) are commercially available. Furthermore, the QEPAS sensor signal is inversely proportional to the QTF resonance frequency f_0. This feature is due to the fact that a QTF with a smaller f_0 will result in a longer effective integration time, which increases the QEPAS signal. In QEPAS, commercially available QTFs with a f_0 of ~32.76 kHz are typically employed, but since 2013 the use of custom QTFs in QEPAS based sensor systems were also reported [19].

In this paper, an EDFA amplified distributed feedback (DFB) diode laser which combines the merits of an EDFA and a diode laser emitting at 1.53 μm with superior output performance was used as the laser excitation source. An ultra-high sensitive NH_3-QEPAS sensor based on the power amplified diode laser and a QTF with a low resonance frequency f_0 of 30.72 kHz was demonstrated for the first time. Wavelength modulation spectroscopy (WMS) and a 2nd harmonic detection technique were used to reduce the sensor background noise. The modulation depth in the WMS QEPAS system was optimized theoretically and verified by the experiments.

2. Experimental setup

2.1 EDFA amplified diode laser characterization

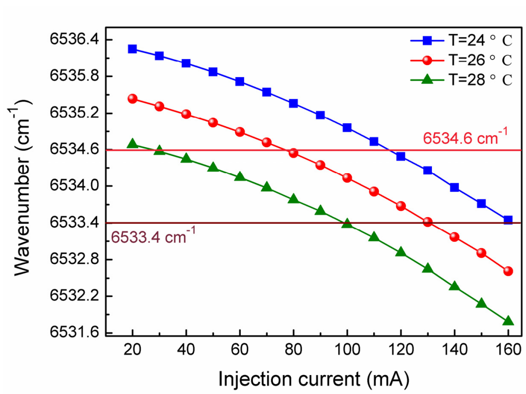

Fig. 1. Current tuning at different operating temperatures of the 1.53 μm CW-DFB diode laser.

A pigtailed, near infrared, continuous wave (CW), DFB diode laser emitting at 1.53 μm was employed as the excitation source. The DFB diode laser was mounted in a 14-pin butterfly package that included a thermoelectric controller (TEC). The laser output wavelength was tuned by controlling the temperature of the TEC and the injection current. The emission spectrum was measured by a laser wavelength meter with a resolution of 0.2 pm (Model No. 721A, Bristol). The measured results are shown in Fig. 1. The laser can cover two NH_3 absorption lines located at 1530.33 nm (6534.6 cm^{-1}) and 1530.60 nm (6533.4 cm^{-1}), respectively, based on the HITRAN 2008 database.

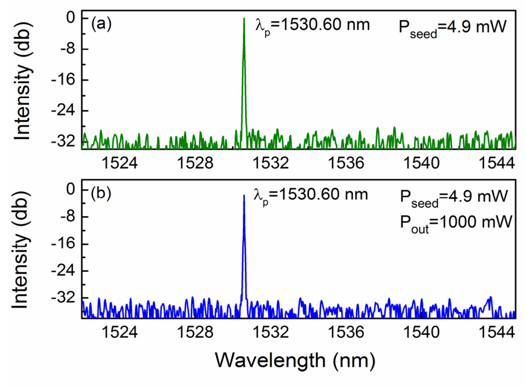

Fig. 2. Near–infrared diode laser emission spectrum: (a) Seed diode laser with a 4.9 mW output power; (b) EDFA amplified diode laser with a 1000 mW output power.

The diode laser emission spectrum has a signal-to-noise ratio of > 30 dB, which can be found in Fig. 2(a). The output of the diode laser was sent to the EDFA for power amplification. The EDFA offers an adjustable measured output power from 50 mW to 1000 mW at the same wavelength as the seed laser. The EDFA consisted of two stages, a preamplifier and a power amplifier, for power scaling. An erbium (Er^{3+})-ytterbium (Yb^{3+}) co-doped fiber was used in the EDFA in order to increase the pumping efficiency. Furthermore, Er^{3+} was sensitized by means of Yb^{3+} co-doping. Amplified spontaneous emission (ASE) of the gain fiber must be minimized in order to reduce the noise level of the amplified diode laser. This was accomplished by means of a narrow-band filter with a center wavelength of 1530.33 nm and transmission bandwidth of 1 nm. The output spectrum of the EDFA is shown in Fig. 2(b). From Fig. 2(b), it can be seen that with a 4.9 mW input, an output power of 1000 mW with a signal-to-noise ratio of ~30 dB for the EDFA amplified laser was obtained.

2.2 QEPAS sensor configuration

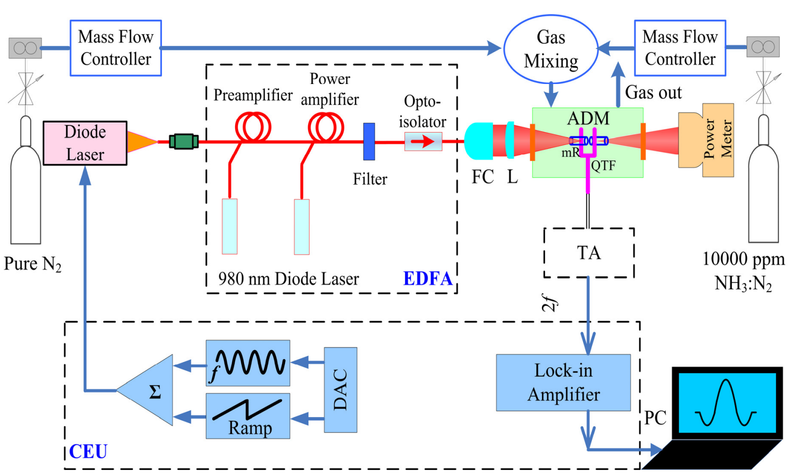

Fig. 3. Schematic configuration of the QEPAS sensor system with an EDFA amplified diode laser.

A schematic of the QEPAS sensor system is shown in Fig. 3. An opto-isolator in the EDFA was used to protect the DFB laser and EDFA against back reflections. The output laser beam from the opto-isolator was collimated by using a fiber collimator (FC) and subsequently focused between the QTF prongs inside an acoustic detection module (ADM) by means of a plano-convex CaF_2 lens (L) with a 40 mm focal length. A QTF with f_0 of 30.72 kHz was employed as the acoustic transducer. A significant enhancement of the QEPAS signal can be achieved when two metallic tubes acting as micro-resonators (mRs) are added to the QTF sensor architecture [20–22]. The optimum length L of metallic tubes should be in the range of $\lambda_s/4<L<\lambda_s/2$, where λ_s is the sound wavelength. For a QTF with f_0 of 30.72 kHz, the optimum length should be 2.8 mm<L<5.5 mm. In this experiment, the length and inner diameter of stainless tubes were selected to be 4 mm and 0.5 mm respectively in order to constitute the mR. The gaps between the QTF and mR tubes were chosen to be 25 µm. The laser beam was directed to an optical power meter for alignment verification of the sensor system after it passed through the ADM. Modulation of the laser current for WMS was performed by applying a sinusoidal dither to the direct current ramp of the diode laser at half of the QTF resonance frequency ($f = f_0/2 \approx 15.36$ kHz). The piezoelectric signal generated by the QTF was detected by a low noise transimpedance amplifier (TA) with a 10 MΩ feedback resistor and converted into a voltage, which was transferred to a custom built control electronics unit (CEU). The CEU provides the following three functions: 1) measurement of the QTF parameters, i.e. the quality factor Q, dynamic resistance R, and resonant frequency f_0; 2) modulation of the laser current at the frequency $f = f_0/2$; and 3) measurement of the $2f$ component generated by the QTF. The NH_3-QEPAS sensor performance was evaluated at different NH_3 concentrations. Two mass flow controllers with a mass flow uncertainty of 3% were used to dilute 10000 ppmv (parts in 10^6 by volume) NH_3 in nitrogen (N_2) and to control the flow rate at 120 ml/min.

3. Theoretical optimization of WMS

When a laser is modulated by an external sinusoidal current, $I = I_0 \cos(\omega_m t)$, both of the laser wavelength and output power are modulated with a phase shift ϕ between them [23,24].

$$v = \overline{v} - \delta_v \cos(\omega_m t + \phi) \tag{1}$$

$$\begin{aligned} P(v) &= P(\overline{v}) + \Delta P(\delta_v)\cos(\omega_m t) \\ &= P_0(1 + p_\Omega \overline{x} + p_\omega m \cos(\omega_m t)) \end{aligned} \tag{2}$$

where $\overline{v}$ is the central wavenumber of laser, δ_v and ΔP are the magnitudes of wavenumber and laser power modulation, respectively. P_0 is the laser power at the gas absorption line center. The parameters, p_Ω and p_ω are the laser power coefficients for scanning (slow ramp) at a frequency ϕ and fast modulation (sinusoidal current) at a frequency ω_m, respectively. The wavenumber $\overline{x}=(\overline{v}-v_0)/\gamma$ is the non-dimensional wavenumber deviation from the line center v_0, $M=\delta_v/\gamma$ is the modulation depth coefficient and γ is the absorption line width. The absorption coefficient can be expressed by following expression:

$$\alpha(v) = CN_0 Sg(v) = \frac{CN_0 S}{\pi\gamma} \cdot \frac{1}{1+\left[(v-v_0)/\gamma\right]^2} = \alpha_0 \frac{1}{1+x^2} \tag{3}$$

where C is the gas concentration, N is the total molecular density, S is the absorption line intensity, $g(v)$ is the normalized line shape function, α_0 is absorption coefficient at the line center and $x=(v-v_0)/\gamma$ is the non-dimensional laser wavenumber. x can be also expressed as follows:

Optics EXPRESS

$$x = \bar{x} - M\cos(\omega_m t + \phi) \tag{4}$$

The absorption coefficient can be rewritten and expanded into a Fourier series by Eq. (5):

$$\begin{aligned}\alpha(\bar{x}) &= \alpha_0 \frac{1}{1+\left(\bar{x} - M\cos\left(\omega_m t + \phi\right)\right)^2} \\ &= \alpha_0\left[H_0(\bar{x}) + \sum_{n=1}^{\infty} H_1(\bar{x})\cos\left(n\omega_m t + n\phi\right)\right]\end{aligned} \tag{5}$$

where $H_0(\bar{x})$ and $H_n(\bar{x})$ are the harmonic coefficients expressed as Eqs. (6) and (7):

$$H_0(\bar{x}) = \frac{1}{\pi}\int_0^{\pi} \frac{1}{1+\left(\bar{x} - M\cos(\theta)\right)^2} d\theta \tag{6}$$

$$H_n(\bar{x}) = \frac{2}{\pi}\int_0^{\pi} \frac{\cos(n\theta)}{1+\left(\bar{x} - M\cos(\theta)\right)^2} d\theta \tag{7}$$

The second harmonic acoustic signal is used to retrieve gas concentrations when applying the WMS technique and the signal S_{2f} is given by Eq. (8):

$$\begin{aligned}S_{2f}(v) &= kC_{cell}\left[\alpha(v)P(v)\right]_{2f} \\ &= kC_{cell}\alpha_0 P_0\left[\left(1+p_\Omega \bar{x}\right)H_2\cos\left(2\omega_m t + 2\phi\right)\right]\end{aligned} \tag{8}$$

where C_{cell} is the constant for the sensor system, k is the conversion constant of the system and $f = \omega_m/2\pi$ is the modulation frequency. The second harmonic acoustic coefficient in the bracket of Eq. (8) can be used to do a theoretical simulation for S_{2f} and hence determine the optimum modulation depth coefficient. The selected NH_3 absorption line located at 6533.4 cm^{-1} and the calculated results are shown in Fig. 4.

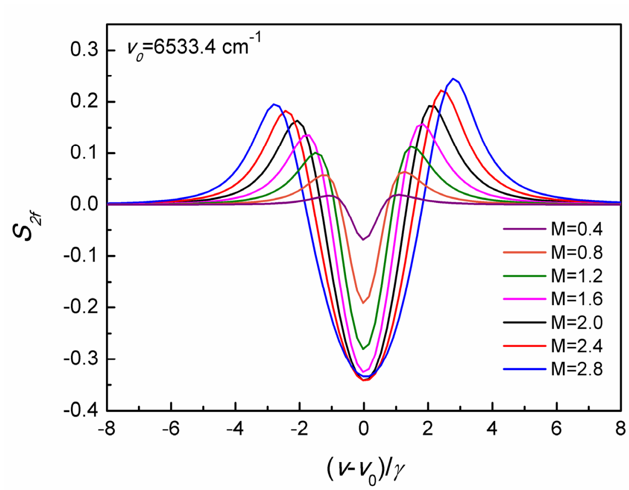

Fig. 4. Second harmonic signal S_{2f} as a function of the modulation depth coefficient.

Optics EXPRESS

4. Experimental results and discussion

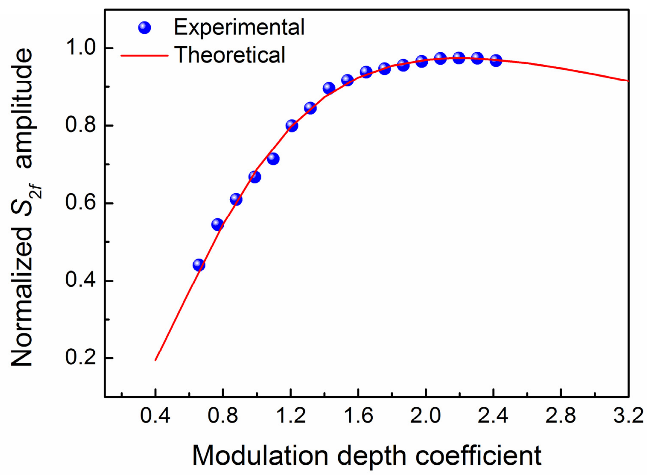

Fig. 5. Normalized S_{2f} signals as function of the modulation depth coefficient.

The QEPAS sensor performance using a diode laser without an EDFA was evaluated first. The laser wavelength modulation depth coefficient should be optimized in order to improve the $2f$ QEPAS signal amplitude. First, the NH_3 6533.4 cm^{-1} absorption line was investigated. The line width parameter γ is 0.0856 cm^{-1} based on the HITRAN 2008 database [25]. The dependence of the QEPAS signal amplitude as a function of the laser wavelength modulation depth coefficient is depicted in Fig. 5. The calculated results and experimental investigations are plotted as a red line and as blue dots, respectively. The experimental results are in agreement with the simulation. The QEPAS signal amplitude increases with the modulation depth coefficient, but when the modulation depth coefficient was higher than 2.2, no further increase was observed. Therefore the optimum modulation depth coefficient was found to be 2.2 and in wavenumber the modulation depth was 0.188 cm^{-1}. Similarly, the optimum modulation depth in wavenumber was found to be 0.196 cm^{-1} for the NH_3 6534.6 cm^{-1} absorption line. Therefore, in the following experiments, the optimum modulation depth of 0.188 cm^{-1} and 0.196 cm^{-1} was used for the two absorption lines located at 6533.4 cm^{-1} and 6534.6 cm^{-1}, respectively.

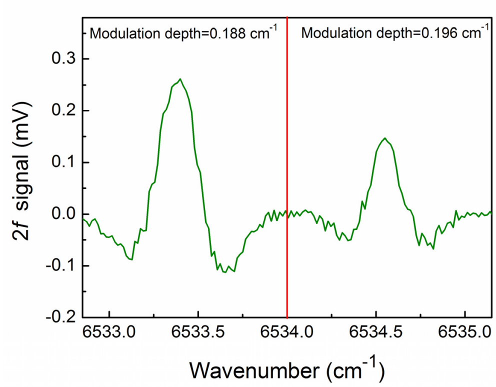

Fig. 6. NH_3-QEPAS signals for two absorption lines located at 6533.4 cm^{-1} and 6534.6 cm^{-1} with the optimum modulation depth.

The 2*f* signals for the two absorption lines of 6533.4 cm^{-1} and 6534.6 cm^{-1} with the optimum modulation depth was investigated and is shown in Fig. 6. It can be see that the two lines were free from spectral interference with each other and the 2*f* signal for absorption line located at 6533.4 cm^{-1} was stronger than that of the 6534.6 cm^{-1} line. Therefore, the absorption line of 6533.4 cm^{-1} was adopted in the following investigations in order to obtain the optimum detection sensitivity.

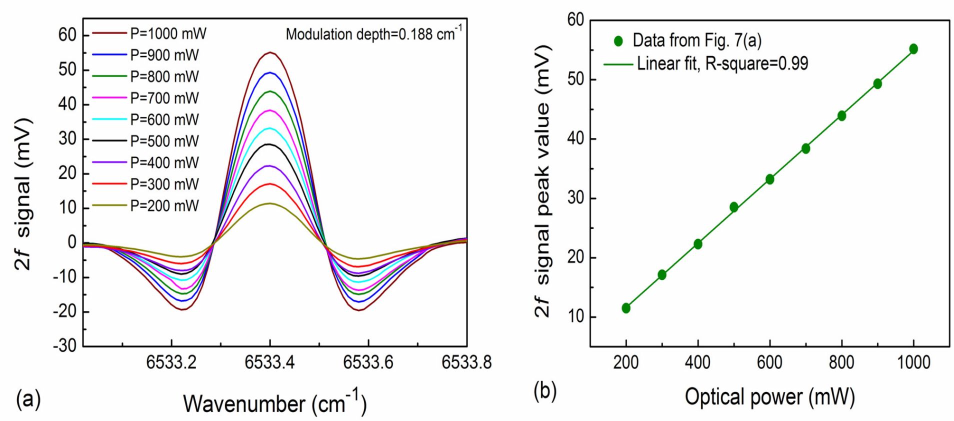

Fig. 7. QEPAS signal. (a) Different optical power levels with an optimum modulation depth of 0.188 cm^{-1}. (b) QEPAS signals peak value as a function of optical power.

The QEPAS sensor performance was further investigated using EDFA amplified DFB diode laser excitation. The 6533.4 cm^{-1} absorption line with an optimum modulation depth of 0.188 cm^{-1} was used. The optical power of the amplified diode laser was varied from 200 mW to 1000 mW. The QEPAS sensor signal amplitude as a function of laser optical power is shown in Fig. 7(a) and Fig. 7(b). It can be seen that the QEPAS signal amplitude improved with increasing laser optical power. The peak values of QEPAS signal are depicted in Fig. 7(b) and a linear fitting procedure was applied. The calculated R-square value, which represents how well the regression line approximates to real data points, is equal to ~0.99. This implies that the sensor system exhibits an excellent linearity response of optical power levels. No saturable absorption effects were observed in this investigation. This means that the NH_3-QEPAS signal amplitude can be even further improved if a higher power EDFA is used.

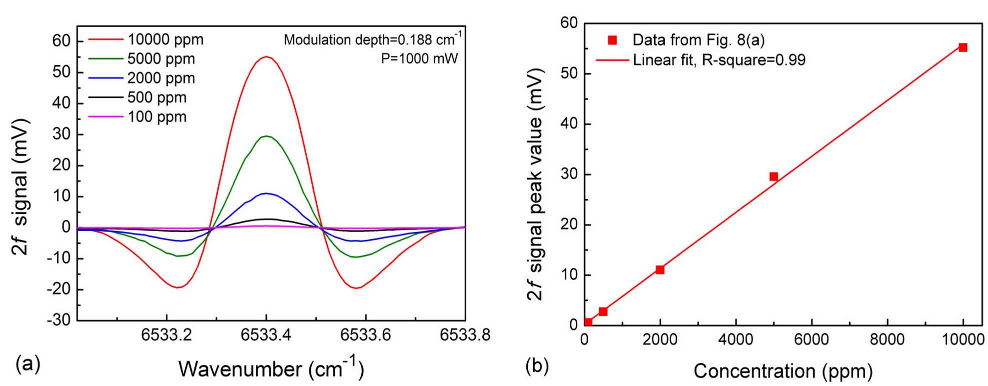

Fig. 8. QEPAS signal. (a) Different NH_3 concentration levels with an optimum modulation depth of 0.188 cm^{-1}. (b) QEPAS signals peak value as a function of NH_3 concentration.

Optics EXPRESS

To verify the linear concentration response of the QEPAS based NH_3 sensor platform, a 10,000 ppm NH_3:N_2 gas mixture was diluted with dry N_2 down to 100 ppm NH_3 concentration levels as depicted in Fig. 8(a). The laser optical power was set to a maximum value of 1,000 mW. The measured QEPAS signal peak value as a function of NH_3 concentrations is plotted in Fig. 8(b). The calculated R-square value is equal to ~0.99 after a linear fitting procedure, which indicates that the sensor system has an excellent linearity response of the NH_3 concentration levels. When the ADM was flushed with ultra high purity N_2 the background signal was determined. Based on the measured signal and noise, the 1σ minimum detection limit (MDL) of the NH_3-QEPAS sensor of 418.4 ppbv was obtained for a 1 sec time constant of the lock-in amplifier. The corresponding normalized noise equivalent absorption coefficient (NNEA) was 3.83×10^{-8} $cm^{-1}W/\sqrt{Hz}$.

5. Conclusions

In conclusion, an ultra-high sensitive QEPAS based NH_3 sensor was demonstrated in this paper. A QTF with low resonance frequency f_0 of 30.72 kHz resulting in a longer effective integration time was used as an acoustic wave transducer. A pigtailed, near infrared, CW, TEC, DFB telecommunication diode laser emitting at 1.53 µm was employed as the laser excitation source. An EDFA was used to increase the optical power up to 1,000 mW. The low f_0 of QTF and the high laser power increase the QEPAS signal level. WMS and a 2nd harmonic detection technique were used to reduce the sensor background noise and simplify the data processing. The modulation depth in the WMS QEPAS system was optimized theoretically and verified experimentally. For the NH_3 sensor system operating at atmospheric pressure, a 418.4 ppbv MDL at 6533.4 cm^{-1} was achieved when the modulation depth was set to the optimum value of 0.188 cm^{-1}. The ppb-level detection sensitivity verified that the design of the reported QEPAS method demonstrated a significantly enhanced sensor system performance. The MDL of NH_3-QEPAS sensor can be further improved if an absorption line with a stronger line strength than the adopted 6533.4 cm^{-1} was used. Furthermore, when an EDFA with an even higher output power and a QTF with a lower f_0 are used the sensor capability can be significantly improved.

Funding

National Natural Science Foundation of China (NSFC) (Grant No. 61505041); Natural Science Foundation of Heilongjiang Province of China (Grant No. F2015011); China Postdoctoral Science Foundation Financial Grant (Grant No. 2014M560262 and 2015T80350); Heilongjiang Province Postdoctoral Foundation Financial Grant (Grant No. LBH-TZ0602 and LBH-Z14074); Fundamental Research Funds for the Central Universities; Application Technology Research and Development Projects of Harbin (No. 2016RAQXJ140); US National Science Foundation ERC MIRTHE award; Welch Foundation Grant C-0586/R4925U.